NASA TECHNICAL MEMORANDUM

NASA TM X-3429

NASA TM X-3429

HOT HARDNESS OF NICKEL-RICH NICKEL-CHROMIUM-ALUMINUM ALLOYS

Stanley R. Levine

Lewis Research Center
and U.S. Army Air Mobility R&D Laboratory
Cleveland, Ohio 44135

NATIONAL AERONAUTICS AND SPACE ADMINISTRATION • WASHINGTON, D. C. • OCTOBER 1976

1. Report No. NASA TM X-3429	2. Government Accession No.	3. Recipient's Catalog No.
4. Title and Subtitle HOT HARDNESS OF NICKEL-RICH NICKEL-CHROMIUM-ALUMINUM ALLOYS		5. Report Date October 1976 6. Performing Organization Code
7. Author(s) Stanley R. Levine		8. Performing Organization Report No. E-8750
9. Performing Organization Name and Address Lewis Research Center and U.S. Army Air Mobility R&D Laboratory Cleveland, Ohio 44135		10. Work Unit No. 505-01 11. Contract or Grant No.
12. Sponsoring Agency Name and Address National Aeronautics and Space Administration Washington, D.C. 20546		13. Type of Report and Period Covered Technical Memorandum 14. Sponsoring Agency Code
15. Supplementary Notes		

16. Abstract

Rockwell A hardness of cast nickel-chromium-aluminum (NiCrAl) alloys was examined from ambient to 1150 K and compared to cast NiAl and IN-100. Alloy constitution was either γ, γ', $+\gamma$, or $\gamma + \beta + \alpha + \gamma'$. Below 1000 K β-containing NiCrAl alloys have hardnesses comparable to IN-100; above 1000 K they soften faster than IN-100. At 1150 K the hardness of β-containing NiCrAl alloys decreases with increasing β-content. The β-containing NiCrAl alloys were harder than β-NiAl. The ultimate tensile strengths σ_u of the NiCrAl alloys were estimated from hardness by the relation $\sigma = 8.55\times10^{-2}\,\bar{R}_A^2 + 10.1\,\bar{R}_A$ (MN/m^2), which was developed in this study for nickel-base alloys. The effects of NiCrAl coatings on strength and fatigue life of cooled turbine components were deduced.

17. Key Words (Suggested by Author(s))	18. Distribution Statement
Hot hardness Nickel alloys Coatings	Unclassified - unlimited STAR Category 26

19. Security Classif. (of this report)	20. Security Classif. (of this page)	21. No. of Pages	22. Price*
Unclassified	Unclassified	18	$3.50

* For sale by the National Technical Information Service, Springfield, Virginia 22161

HOT HARDNESS OF NICKEL-RICH NICKEL-CHROMIUM-ALUMINUM ALLOYS

by Stanley R. Levine

Lewis Research Center and
U. S. Army Air Mobility R&D Laboratory

SUMMARY

The Rockwell A hardness of cast nickel-rich nickel-chromium-aluminum (NiCrAl) alloys representative of overlay coating compositions was examined from room temperature to 1150 K. Alloy constitution was either γ, $\gamma' + \gamma$, γ-rich $\gamma + \beta + \alpha + \gamma'$, or β-rich $\beta + \gamma + \alpha + \gamma'$ phases. The hot hardness behavior of these alloys was compared to that of cast stoichiometric NiAl(β) and the cast nickel-base superalloy IN-100. Up to about 1000 K the β-containing NiCrAl alloys had hardness values comparable to IN-100; above this temperature they soften more rapidly with increasing temperature than IN-100. At 1150 K the hardness of β-containing alloys decreased with increasing β-content. The β-containing NiCrAl alloys were harder than β-NiAl. The knee in the hardness as a function of temperature relations for the NiCrAl alloys is about 200 K above the 725 K DBTT for NiAl, and the temperature dependence of hardness is weaker for the NiCrAl alloys than for NiAl below the break temperature. The relation $\sigma_u = 8.55\times10^{-2}\,\bar{R}_A^2 + 10.1\,\bar{R}_A$ (in MN/m^2) was developed in this study to convert Rockwell A hardness $\bar{R}_A$ to ultimate tensile strength σ_u for ductile nickel-base alloys. The effects of NiCrAl coatings on strength and fatigue life of cooled turbine components were deduced.

INTRODUCTION

One of the primary attributes desired from protective coatings applied to superalloy gas turbine blades or vanes is that they increase the tolerance of the components to thermal fatigue cycling. The ability of a coating to extend thermal fatigue life may be viewed from either an environmental interaction or from a fatigue standpoint (ref. 1). From the environmental viewpoint a protective coating provides a relatively homogeneous oxidation resistant layer which isolates the alloy from the environment. Thus, alloy grain boundaries, which are generally more susceptible to oxidation than the bulk alloy,

cannot serve as environmentally triggered surface crack initiation sources (ref. 1). In terms of fatigue, one of the most important properties is ductility, which determines life in the low-cycle fatigue range (ref. 2). A ductile coating can extend life by inhibiting crack initiation from the surface. This point is illustrated by the behavior of the aluminide class of coatings. Aluminide coatings extend the thermal fatigue lives of coated superalloys when thermal strains peak at relatively high temperatures (above 1000 K) where the ductility of NiAl is adequate (refs. 3 and 4). This condition is usually met for uncooled airfoils. In cooled turbine components thermal strains are generally smaller (ref. 4), but they peak at lower temperatures. Here, aluminide coatings can have a detrimental effect on thermal fatigue life (ref. 4). Consequently, more ductile, highly environmental resistant coatings of the NiCrAl or CoCrAl overlay type are finding increased usage on the air-cooled airfoils of advanced gas turbines.

Practical thermal fatigue lives for turbine airfoils are in the neighborhood of 1000 to 10 000 cycles. In this life range, the elastic strain range is a significant fraction of the total strain range. Thus, in addition to ductility, the elastic modulus and ultimate tensile strength can significantly influence thermal fatigue life. Specifically, a high ultimate tensile strength/elastic modulus ratio is desired for long life (ref. 2). In addition, this ratio determines the high-cycle fatigue life of coated blade roots.

The direct purpose of this study was to examine the effect of composition on the hardness of alloys in the nickel-rich corner of the NiCrAl ternary system. Hot hardness can be related to ultimate tensile strength (ref. 5) - an important variable in thermal fatigue and high-cycle fatigue life considerations. A second purpose of this study was to draw some conclusions about NiCrAl coating composition effects on thermal and high-cycle fatigue life of superalloys using the hardness data measured and an estimate of the elastic modulus. Finally, the contribution of thick (0.013 cm) overlay coatings to the local section strength of thin-walled (0.05 to 0.13 cm) air-cooled turbine components was deduced from the hot hardness data.

This study is part of a larger program directed at obtaining a better overall understanding of NiCrAl and CoCrAl systems now in use or anticipated for use in overlay coatings and as matrix alloys. Coefficient of thermal expansion (ref. 6), cyclic oxidation (ref. 7), hot corrosion, diffusional stability, and mechanical properties are being studied so that optimum compositions can be rapidly and accurately selected for specific applications.

EXPERIMENTAL PROCEDURE

Materials Preparation

Nine NiCrAl alloys were vacuum melted in zirconia crucibles and cast in zirconia shell molds. Further fabrication details are given by Barrett and Lowell (ref. 7). Alloy chemistries determined by atomic absorption spectroscopy are listed in table I. In addition, stoichiometric NiAl was prepared by electron beam melting in a copper mold. Cast IN-100 and wrought Inconel 600 and Hastelloy X were used as reference materials having well characterized tensile properties.

The surface quality of the wrought alloys, Hastelloy X and Inconel 600, was sufficient for testing in the as-received condition. The cast alloys were prepared for hardness testing by wet polishing through 600 grit silicon carbide paper. All specimens were at least 0.15 centimeter thick.

Hardness Testing

Rockwell A hardness was measured with a standard hardness tester adapted to accommodate a nitrogen purged resistance heated tube furnace as shown in figure 1 (ref. 8). The specimen with a stainless steel sheathed Chromel-Alumel thermocouple attached at the bead by a spot weld was placed on a ceramic pedestal located at the center of the furnace. The furnace assembly was moved by a screw driven mechanical stage so that evenly spaced indentations about 0.15 centimeter apart could be made. Hardness indentations were made with a high-temperature spheroconical penetrator driven by a 60-kilogram major load. For each indentation the major and minor loads were applied for a constant time. The instrument was calibrated at room temperature prior to each run with standard calibration blocks of $R_A = 73.0 \pm 0.5$, $R_A = 63.0 \pm 0.5$, and $R_A = 50.0 \pm 0.8$. At least two and in some cases up to five readings were made at each temperature after the furnace temperature stabilized. Measurements were made over the range from room temperature to 1150 K.

Determination of Alloy Constitution

The phases present in the as-cast alloys were determined by metallographic examination at ×450 after the polished sections were immersion etched with 33 HNO_3 - 33 HCl - 33 glycerol - 1HF by volume. The as-cast structure was compared with the equilibrium phases present after an 1370 K, 500-hour anneal followed by an air cool.

Phases present in the annealed alloys were confirmed by electron beam microprobe analyses. The volume fractions of the β-phase were determined with an image analyzing computer.

RESULTS AND DISCUSSION

Constitution of the NiCrAl Alloys

The phases present in the cast NiCrAl alloys are listed in table I. The major phase is listed first. Nickel solid solution is denoted by γ, γ' designates the Ni_3Al structure, β designates the NiAl structure, and α the chromium solid solution. Recognizing that the as-cast alloys are not at equilibrium, their constitutions still compare favorably with the 1000° C equilibrium diagram of Taylor and Floyd (ref. 9). The major deviation from the 1000° C diagram, the presence of γ' in alloys 3 and 4, is consistent with Taylor and Floyd's 850° C equilibrium diagram (ref. 9). The γ'-phase precipitated as the castings slowly cooled. Precipitation of γ' was, in some measure, due to coring in alloy 4.

The alloys can be divided into four groups based on the phases present: γ (alloy 7); $\gamma + \gamma'$ (alloys 3, 4, and 9); predominantly γ with β, α, and γ' present (alloys 1, 2, and 8); and predominantly β with γ and α the principal minor phases (alloys 5 and 6). Alloys in the two latter groups will be referred to as $\gamma + \beta$ and $\beta + \gamma$, respectively. Photomicrographs of an alloy from each of the last three groups are shown in figure 2.

One should note at this point that the alloys exhibit a typical coarse cast structure whereas overlay coatings generally consist of a dispersion of fine second phase particles in a continuous γ matrix phase. This disparity in structure is most pronounced for alloys 2 and 6 which consist of dendritic β-phase in a γ-matrix. Hardness indentations were much larger than the dendrites. For example, alloy 6 illustrated in figure 2(c) had indentation diameters which ranged from about 320 micrometers at room temperature to about 910 micrometers at 1145 K. Thus, each hardness reading is indicative of the bulk material rather than an individual phase.

Hot Hardness of the NiCrAl Alloys

The average hardness data for the four types of NiCrAl alloys are presented in figures 3(a) to (d) as functions of temperature. They are grouped according to the major phases present: figure 3(a), γ; 3(b), $\gamma + \gamma'$; 3(c), $\gamma + \beta$; and 3(d), $\beta + \gamma$. In each case the data for IN-100 are plotted for comparison. The β-NiAl alloy (fig. 3(d) could not sustain indentations at temperatures above 400 K without fracturing. The plotted lines

for NiAl are based on the Vickers hardness data of Westbrook (ref. 10) converted to Rockwell A hardness (ref. 11). The agreement between the limited data obtained in this study and the converted data from Westbrook is good. The hardness as a function of temperature data for each alloy can be represented by pairs of straight lines - a low temperature and a high temperature segment. The data for each alloy were fit to pairs of linear equations of the form $\overline{R}_A = mT + b$ by linear regression. The pair of lines with the maximum average correlation coefficient was selected as the best fit to the data.

The γ alloy is far softer than IN-100 over the entire temperature range and exhibits a more rapid rate of hardness loss than IN-100 at the higher temperatures (fig. 3(a)). The composition of this alloy can be considered representative of a severely depleted overlay coating. The $\gamma + \gamma'$ alloys 3 and 9 behave like IN-100 over the entire temperature range (fig. 3(b)) although they are about 10 percent softer due to the absence of carbides and the additional solid solution strengtheners found in IN-100. Up to about 900 K they exhibit an increase in hardness with increasing temperature as expected for alloys containing a high volume fraction of γ' (ref. 12). Alloy 4 does not exhibit this strengthening behavior, but behaves more like the γ alloy (fig. 3(a)) because the γ' was mainly associated with coring and the overall volume fraction of γ' was quite low. Here the γ' strengthening did not offset the softening of γ. At temperatures above the break or knee in the hardness-temperature curve alloy 9 softens at about the same rate as IN-100. Alloy 3 softens more rapidly than alloy 9 above 1000 K due to its higher chromium content and lower γ' volume fraction as indicated in reference 12.

The $\gamma + \beta$ NiCrAl alloys (also containing α and γ') are harder than IN-100 near room temperature (fig. 3(c)). Their hardness decreases with increasing temperature over the entire temperature range examined. Above about 1000 K they soften more rapidly than IN-100.

The $\beta + \gamma$ NiCrAl alloys (fig. 3(d)) behave like their γ-rich counterparts (fig. 3(c)). The β-rich alloys are harder than IN-100 up to about 950 K. Above this temperature they soften more rapidly than IN-100. The β-containing alloys have chemistries representative of as-deposited overlay coatings.

NiAl is harder than IN-100 at low temperatures but softens rapidly. The knee which occurs at about 725 K is associated with a ductile-brittle transition in polycrystalline NiAl (ref. 13). Above the transition temperature NiAl softens more rapidly than IN-100 does above 900 K. The hardness behavior of the alloys examined in this study can be summarized as follows:

Room temperature hardness	$(\beta + \gamma) >$ IN-100 $\approx (\gamma + \beta) \approx \beta > (\gamma' + \gamma) > \gamma$
900 K hardness	IN-100 $\approx (\beta + \gamma) > (\gamma + \beta) > (\gamma' + \gamma) > \beta > \gamma$
1150 K hardness	IN-100 $> (\gamma' + \gamma) > (\gamma + \beta) > (\beta + \gamma) > \beta > \gamma$
Slope (RT to knee)	IN-100 $> (\gamma' + \gamma) > 0 > (\gamma + \beta) > \gamma > (\beta + \gamma) > \beta$
Slope (above knee)	$0 >$ IN-100 $> (\gamma' + \gamma) > \beta > \gamma \approx (\gamma + \beta) > (\beta + \gamma)$

Considerable additional hardening of γ is possible by further solid solution strengthening by chromium and aluminum.

The hot hardness behavior of the γ-rich β-containing NiCrAl alloys and the β-rich NiCrAl alloys differs considerably from the behavior of stoichiometric β (figs. 3(c) and (d)). This is so even for alloy 5 which contains about 80 volume percent β. The difference does not appear to be due to variations in the aluminum content of β-NiAl. According to Westbrook (ref. 10), in going from stoichiometric β to Ni - 39 atom percent Al β-phase the ductile-brittle transition temperature increases about 100 K. Also, the hardness below the transition temperature increases by about 50 percent, and there is essentially no effect of composition on change in hardness at temperatures well above the transition temperature. For the NiCrAl alloys the break in the hardness-temperature curves is about 200 K above the ductile-brittle transition temperature for stoichiometric β-NiAl (figs. 3(c) and (d)). Also, the effect of temperature on hardness below the break temperature is considerably weaker than in NiAl. The differences in hardness behavior between the β-containing NiCrAl alloys and NiAl may be due to the presence of the γ-, γ'-, and α-phases in the NiCrAl alloys.

A general correlation of hardness with composition could not be made. There were too few γ and $\gamma + \gamma'$ alloys to make a hardness correlation for these groups; their mechanical behavior is well documented in the literature. A hardness-composition correlation was found for the six β-containing alloys. Their hardness at 1150 K is related to volume percent β as shown in figure 4. Hardness at 1150 K decreases with increasing β content (or increasing aluminum content).

Hardness - Ultimate Tensile Strength Correlation

Rockwell A hardness for the reference alloys IN-100 (295 to 1145 K), Hastelloy X, and Inconel 600 (295 K) are plotted against literature values of ultimate tensile strength (refs. 14 to 16) in figure 5. The relation

$$\sigma_u = 8.55\times10^{-2}\,\overline{R}_A^2 + 10.1\,\overline{R}_A \ \text{MN/m}^2$$

or

$$\sigma_y = 1.24\times10^{-2}\,\overline{R}_A^2 + 1.47\,\overline{R}_A \ \text{ksi}$$

(with $\pm2\sigma$ confidence intervals of 64 MN/m^2 or 9 ksi) provide a good correlation between Rockwell A hardness and ultimate tensile strength. Only the 295 K data point for IN-100 falls outside the $\pm2\sigma$ band. Although a linear equation gave a slightly better fit to the data

it extrapolated to negative values of ultimate tensile strength at low values of R_A and so was discarded. The only expected limitation on the previous relation is that the material must have adequate tensile ductility to sustain a significant amount of tensile plastic deformation. The relation would break down for single-phase polycrystalline NiAl in the vicinity of and below the transition temperature because of its low ductility.

The inference of the ultimate tensile strength of vapor deposited coatings from values computed from hardness measurements on cast alloys carries an element of uncertainty due to the differences in microstructure. Since most of the alloys have a continuous γ matrix and therefore some ductility at all temperatures, the hardness tests on the cast alloys should give reasonable estimates of the ultimate tensile strengths of the fine-grained vapor deposited alloys. Exceptions are β-NiAl as noted earlier and possibly alloy 5 which has a low volume fraction of γ and a continuous β-phase. The uncertainty associated with ultimate tensile strength computed from hardness measurements is probably greatest for these brittle alloys. For a brittle alloy, the hardness measurements would give higher computed ultimate strength values than a tensile test on the same material. For brittle alloys, grain size reduction can result in large increases in fracture stress. The grain size reduction associated with going from a cast to a vapor deposited NiCrAl tends to compensate for the anticipated error resulting from computing the ultimate tensile strength of brittle alloys from Rockwell hardness data.

The hardness data were converted to ultimate tensile strength by using the relations given previously. The average behavior for each alloy class based on phases present at room temperature in the as-cast condition is given in figure 6. From this figure it is apparent that the $\beta + \gamma$ and $\gamma + \beta$ alloys have calculated ultimate tensile strengths comparable to those published for IN-100 and other nickel-base superalloys up to about 1000 K. Above this temperature the β-containing NiCrAl alloys lose strength much more rapidly than does IN-100.

CONCLUDING REMARKS

Elastic Modulus of the NiCrAl Alloys

The modulus of elasticity of alloy 5 was determined at room temperature from the natural frequency of a cantilevered beam of the material. A beam 12.45 millimeters long (l), 0.51 millimeter deep (a), and 3.4 millimeters wide had a natural frequency (f) of 2620 hertz. The modulus of elasticity E is given by (ref. 17)

$$E = \rho \frac{f^2 l^4}{a^2}$$

The density ρ of the alloy is 6.74 grams per cubic centimeter and the computed modulus of elasticity is 1.7×10^5 meganewtons per square meter. The modulus of elasticity of alloy 5 is about 25 percent lower than that of IN-100 (ref. 14). Three point bend tests of IN-100 and the NiCrAl alloys conducted over the temperature range from ambient to 1150 K indicated that the modulus of elasticity of all of the cast NiCrAl alloys in this study are lower than the modulus of IN-100. As a consequence of their lower modulus the β-containing cast NiCrAl alloys have σ_u/E ratios greater than those of random polycrystalline IN-100 up to about 1000 K.

Implications for Fatigue of Turbine Airfoils

Because the σ_u/E ratio for β-containing NiCrAl is higher than the σ_u/E ratio of random polycrystalline IN-100, these alloys, when applied as coatings, would not be expected to be detrimental to the high-cycle fatigue life of a 900 K blade root. The β alloy and the weak γ alloy would probably not perform as well as the β-containing NiCrAl alloys, $\gamma + \gamma'$ alloys, or a stronger γ alloy in the blade root application.

In thermal fatigue considerations of air-cooled turbine blade or vane airfoils with virgin coatings, as represented by the β-containing cast NiCrAl alloys, the σ_u/E term for the coating is again greater than the σ_u/E term for random polycrystalline IN-100 when thermal strains peak below 1000 K. When thermal strains are in the elastic range these coatings would not be expected to be detrimental to the thermal fatigue life of a random polycrystalline turbine airfoil. When plastic strains predominate, coating ductility is of primary concern. It has already been pointed out (ref. 4) that pack aluminide coatings can be detrimental to thermal fatigue life due to their low ductility at low temperatures.

An extreme case of thermal fatigue is coating cracking due to thermal expansion mismatch between the coating and substrate. This question has been considered by Lowell, et al. (ref. 6) for an overlay coating on a $\gamma/\gamma' - \delta$ substrate. For a thermal expansion mismatch of 5×10^{-6} per K between a 0.013 centimeter thick coating and a 0.13 centimeter thick substrate, the coating would sustain a 900 meganewton per square meter upper bound tensile stress on cooling from 1300 to 300 K. From figure 6 it is apparent that the typical overlay coatings can sustain this stress provided their tensile ductility is adequate.

Implications for Cooled Turbine Airfoil Design

The ability of an overlay coating to make a significant contribution to the local section strength of an air-cooled turbine component is an important question. The critical

region near blade midspan is of particular interest. In this region the β-containing NiCrAl overlay coatings can eventually degrade to a weaker γ-phase as a result of oxidation and diffusion. The weak γ condition represents the worst design case. In the case of a 0.13 centimeter thick location a 0.013 centimeter thick coating can make a 10 percent contribution to section strength if the coating strength equals that of the alloy being protected. In the case of a 0.05 centimeter thick section, as might be found near the trailing edge, a 0.013 centimeter thick coating has to have about 40 percent of the strength of the substrate to make a 10 percent contribution to local section strength. In the degraded γ condition the thick overlay coatings add weight to the blade without adding significant strength at temperatures above 1100 K as can be seen from figure 6.

Under transient conditions, critical strains are developed in an air-cooled turbine component when the leading or trailing edge in the midspan region cools to 600 to 800 K. Under these conditions all of the alloys including γ can make a 10 percent strength contribution to a 0.05 centimeter thick section and the β-containing NiCrAl alloys can make a 10 percent strength contribution to a 0.13 centimeter thick section when present as a 0.013 centimeter thick overlay coating (fig. 6). Therefore, in a rigorous thermal fatigue analysis of an air-cooled turbine component, the coating strength should be considered in the analysis of thin section locations.

SUMMARY OF RESULTS

The Rockwell A hardness of nickel-rich NiCrAl alloys, stoichiometric β-NiAl, and IN-100 were examined from room temperature to 1150 K. The following results were obtained:

1. The hardness behavior of the alloys examined in this study can be summarized as follows:

Room temperature hardness	$(\beta + \gamma) >$ IN-100 $\approx (\gamma + \beta) \approx \beta > (\gamma' + \gamma) > \gamma$
900 K hardness	IN-100 $\approx (\beta + \gamma) > (\gamma + \beta) > (\gamma' + \gamma) > \beta > \gamma$
1150 K hardness	IN-100 $> (\gamma' + \gamma) > (\gamma + \beta) > (\beta + \gamma) > \beta > \gamma$
Slope (RT to knee)	IN-100 $> (\gamma' + \gamma) > 0 > (\gamma + \beta) > \gamma > (\beta + \gamma) > \beta$
Slope (knee to 1150 K)	$0 >$ IN-100 $> (\gamma' + \gamma) > \beta > \gamma \approx (\gamma + \beta) > (\beta + \gamma)$

2. The 1150 K Rockwell A hardness of β-containing alloys decreased with increasing β-content.

3. The hardness of the β-containing NiCrAl alloys was greater than that of stoichiometric β-NiAl from room temperature to 1150 K and the knee in the hardness-temperature curve for the NiCrAl alloys occurred about 200 K above the 725 K DBTT of NiAl.

4. The ultimate tensile strength of nickel-base alloys was related to Rockwell A

hardness by

$$\sigma_u = 8.55\times10^{-2}\,\overline{R}_A^2 + 10.1\,\overline{R}_A \quad MN/m^2$$

or

$$\sigma_u = 1.24\times10^{-2}\,\overline{R}_A^2 + 1.47\,\overline{R}_A \quad ksi$$

with a $\pm2\sigma$ confidence interval of 64 MN/m^2 (9 ksi). The relation is expected to be most reliable for ductile alloys.

Lewis Research Center,
National Aeronautics and Space Administration,
and
U.S. Army Air Mobility R&D Laboratory,
Cleveland, Ohio, May 26, 1976,
505-01.

REFERENCES

1. Gell, M; and Duquette, D. J.: The Effects of Oxygen on Fatigue Fracture of Engineering Alloys. International Conference on Corrosion Fatigue: Chemistry, Mechanics and Microstructure. Natl. Assoc. of Corrosion Engrs., 1972, pp. 366-378.

2. Manson, S. S.: Fatigue: A Complex Subject - Some Simple Approximations. Experimental Mechanics, July 1965, vol. 5, no. 7, pp. 193-226.

3. Wells, C. H.; and Sullivan, C. P.: Low-Cycle Fatigue of Udimet 700 at 1700 F. ASM Trans. Quart., vol. 61, Mar. 1968, pp. 149-155.

4. Suciu, S. N.: High Temperature Turbine Design Considerations. SAE Paper 710462, May 1971.

5. Dieter, George E., Jr.: Mechanical Metallurgy, Chapter 11. The Hardness Test. McGraw-Hill Book Co., Inc., New York, 1961, pp. 282-295.

6. Lowell, Carl E.; Garlick, Ralph G.; and Henry, Bert: Thermal Expansion in the Nickel-Chromium-Aluminum and Cobalt-Chromium-Aluminum Systems to 1200° C. NASA TM X-3268, 1975.

7. Barrett, Charles A.; and Lowell, Carl E.: Resistance of NiCrAl Alloys to Cyclic Oxidation at 1100° C and 1200° C. NASA TN D-8255, 1976.

8. Chevalier, James L.; Dietrich, Marshall W.; and Zaretsky, Erwin V.: Short-Term Hot Hardness Characteristics of Rolling-Element Steels. NASA TN D-6632, 1972.

9. Taylor, A.; and Floyd, R. W.: The Constitution of Nickel-Rich Alloys of the Nickel-Chromium-Aluminum System. J. Inst. Metals, vol. 81, 1952-1953, pp. 451-464.

10. Westbrook, J. H.: Temperature Dependence of Hardness of the Equi-Atomic Iron Group Aluminides. J. of the Electrochem. Soc., vol. 103, no. 1, Jan. 1956, pp. 54-63.

11. Standard Hardness Conversion Tables for Metals - ASTM Designation E140-71. 1971 Annual Book of ASTM Standards, Part 31. Am. Soc. for Testing and Materials, pp. 494-495.

12. Decker, R. F.: Strengthening Mechanisms in Nickel-Base Superalloys. Symposium on Steel Strengthening Mechanisms. Climax Molybdenum Co., 1969, pp. 147-170.

13. Ball, A.; and Smallman, R. E.: The Deformation Properties and Electron Microscopy Studies of the Intermetallic Compound NiAl. Acta Met., vol. 14, no. 10, Oct. 1966, pp. 1349-1355.

14. High-Temperature, High-Strength Nickel Base Alloys. 2nd ed., The International Nickel Co., Inc., 1968.

15. Engineering Properties of Inconel Alloy 600. The International Nickel Co., Inc., 1964.

16. Hastelloy Alloy X. Cabot Corp., 1970.

17. Morse, Philip M.: Vibration and Sound. Ch. 4, McGraw Hill Book Co., Inc., 1948.

TABLE I. - ALLOY COMPOSITIONS AND CONSTITUTIONS

Alloy	Ni	Cr	Al	Zr	As-cast phases[a]		Volume, % β
	Composition, wt % (at. %)				Major[b]	Minor	
7	82.5 (78.4)	14.7 (15.8)	2.8 (5.8)	0.016 (-)	γ	-----	---
3	81.3 (74.7)	12.7 (13.2)	6.0 (12.1)	.11 (-)	$\gamma' + \gamma$	-----	---
4	76.7 (70.5)	17.7 (18.4)	5.5 (11.1)	.66 (-)	$\gamma + \gamma'$	-----	---
9	81.6 (73.1)	9.6 (9.7)	8.8 (17.2)	.30 (-)	$\gamma' + \gamma$	-----	---
1	75.0 (66.5)	16.0 (16.0)	9.1 (17.5)	.20 (-)	$\gamma + \beta$	$\gamma' + \alpha$	15
2	75.5 (65.4)	12.8 (12.5)	11.7 (22.0)	.37 (-)	$\gamma + \beta$	$\gamma' + \alpha$	25
8	70.4 (62.3)	20.8 (20.8)	8.8 (16.9)	.039 (-)	$\gamma + \beta$	$\alpha + \gamma'$	20
5	66.0 (54.6)	18.3 (17.1)	15.7 (28.2)	.34 (-)	$\beta + \gamma$	α	80
6	67.9 (57.9)	19.5 (18.8)	12.6 (23.4)	.071 (-)	$\beta + \gamma$	$\alpha + \gamma'$	55
NiAl	68.6 (50.1)	----------	31.4 (49.9)	-------	β	-----	100

Alloy	Ni	Cr	Al	Zr	W	Co	Fe	Mo	Mn	Ti	Si	B	V	C
	Composition, wt %													
IN-100	62.9	9.84	5.50	0.07	---	12.84	0.12	3.01	0.01	4.41	0.03	0.015	1.03	0.18
Hastelloy X[c]	47.3	22.0	----	----	0.6	1.5	18.5	9.0	.50	----	.50	-----	----	.10
Inconel 600[c]	76.6	15.8	----	----	---	-----	7.2	----	.20	----	.20	-----	----	.04

[a]Listed in order of amount of phase present.
[b]Alloys designated by major phases in text.
[c]Nominal composition.

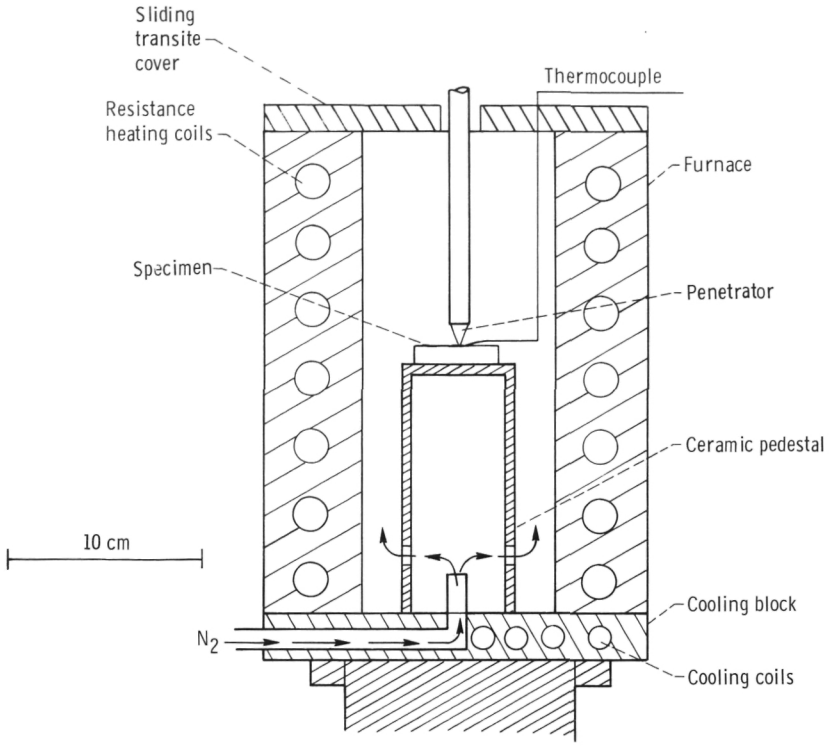

Figure 1. - Cross section of hot hardness tester (ref. 8).

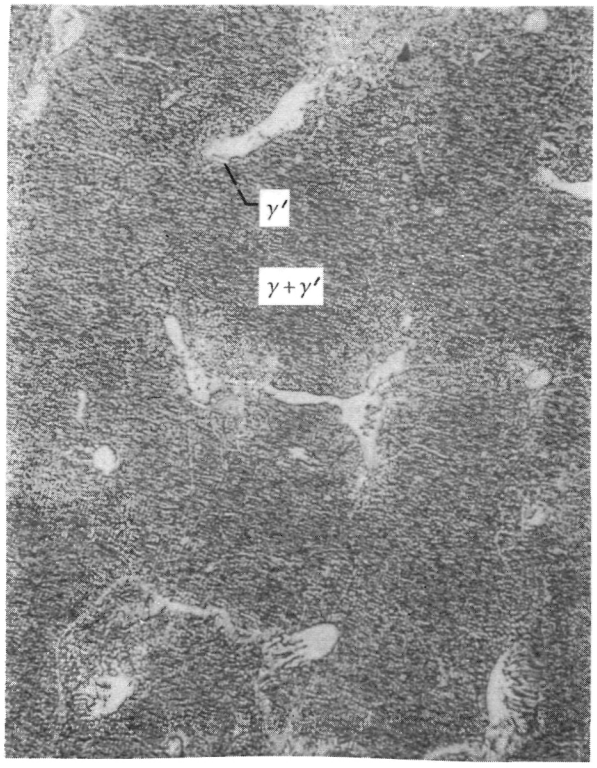

(a) Alloy 9: Ni-9.6Cr-8.8Al; $\gamma'+\gamma$.

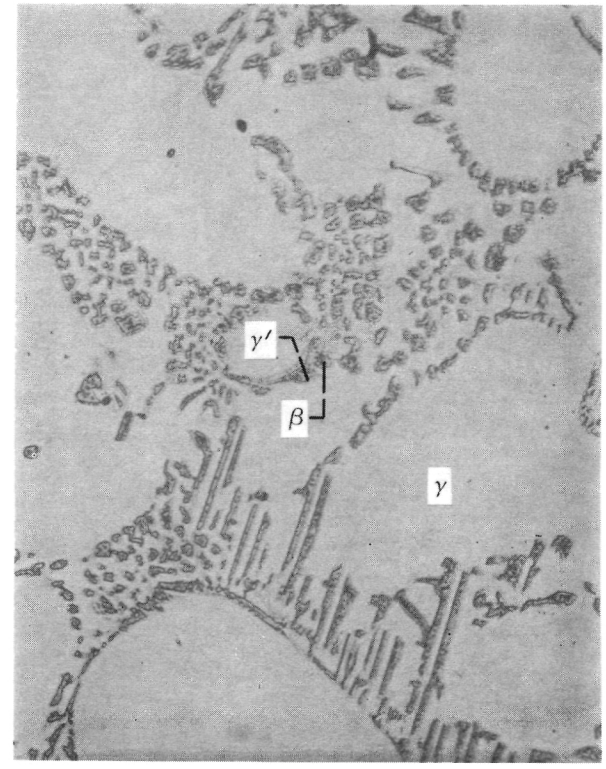

(b) Alloy 8: Ni-20.8Cr-8.8Al; γ predominant with β, α, and γ' present.

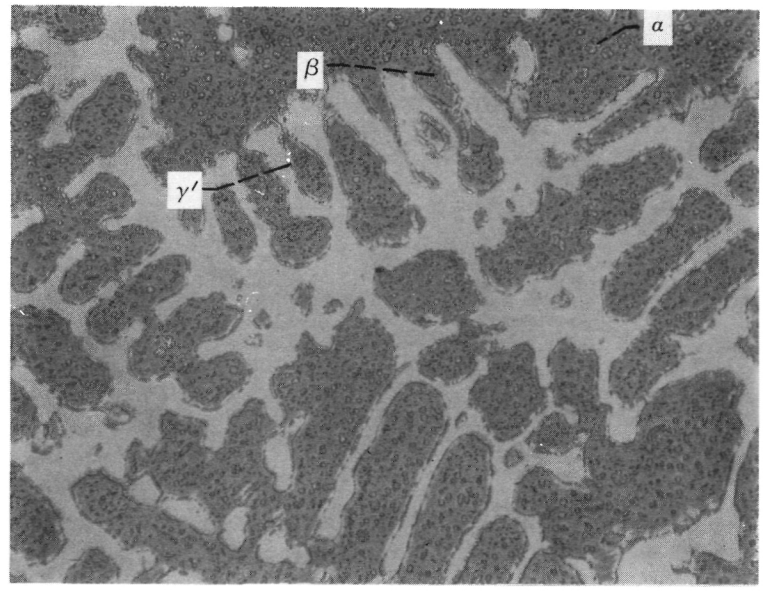

(c) Alloy 6: Ni-19.5Cr-12.6Al; β predominant with γ, α, and γ' present.

Figure 2. - Photomicrographs of three classes of NiCrAl alloys (in wt %).

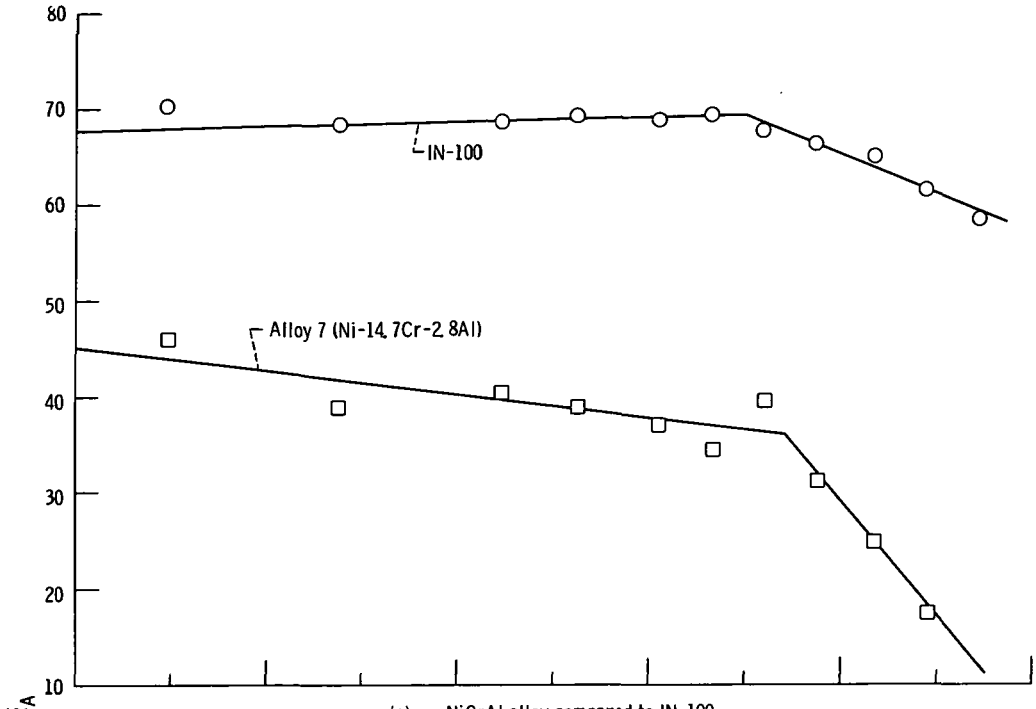

(a) γ - NiCrAl alloy compared to IN-100.

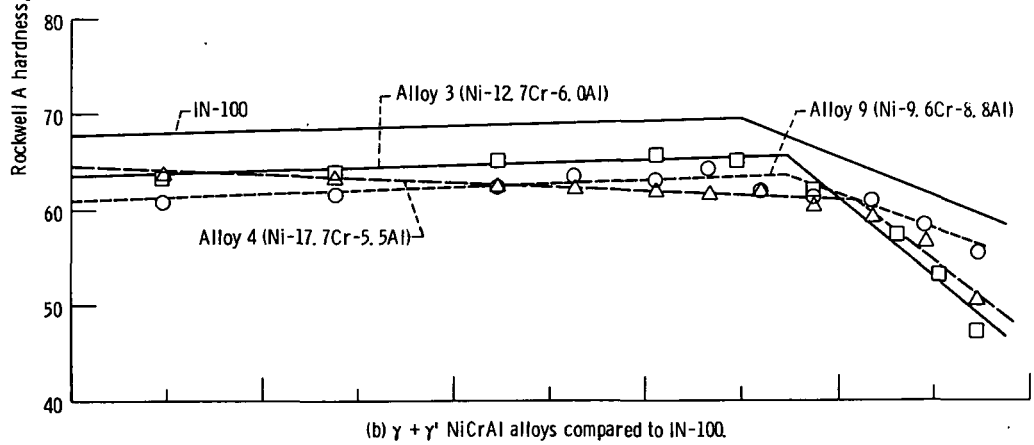

(b) γ + γ' NiCrAl alloys compared to IN-100.

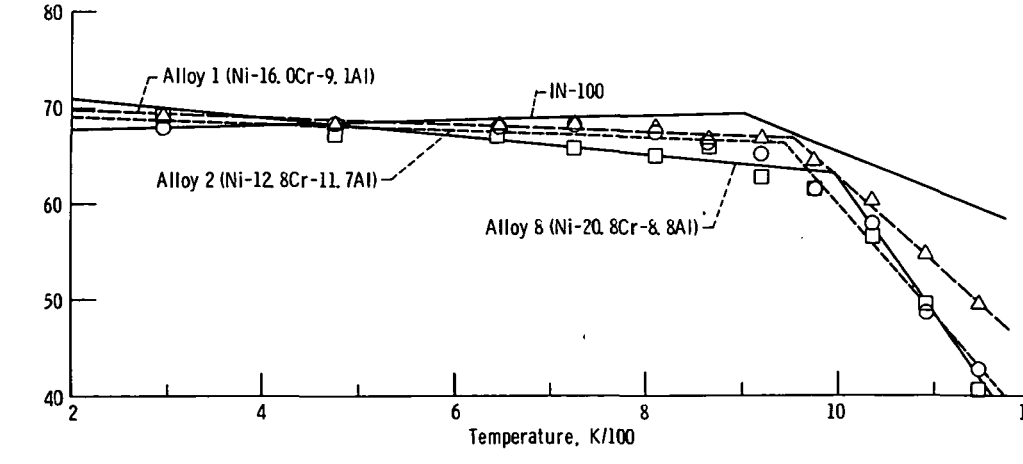

(c) γ-rich γ + β NiCrAl alloys compared to IN-100.

Figure 3. - Hot hardness data.

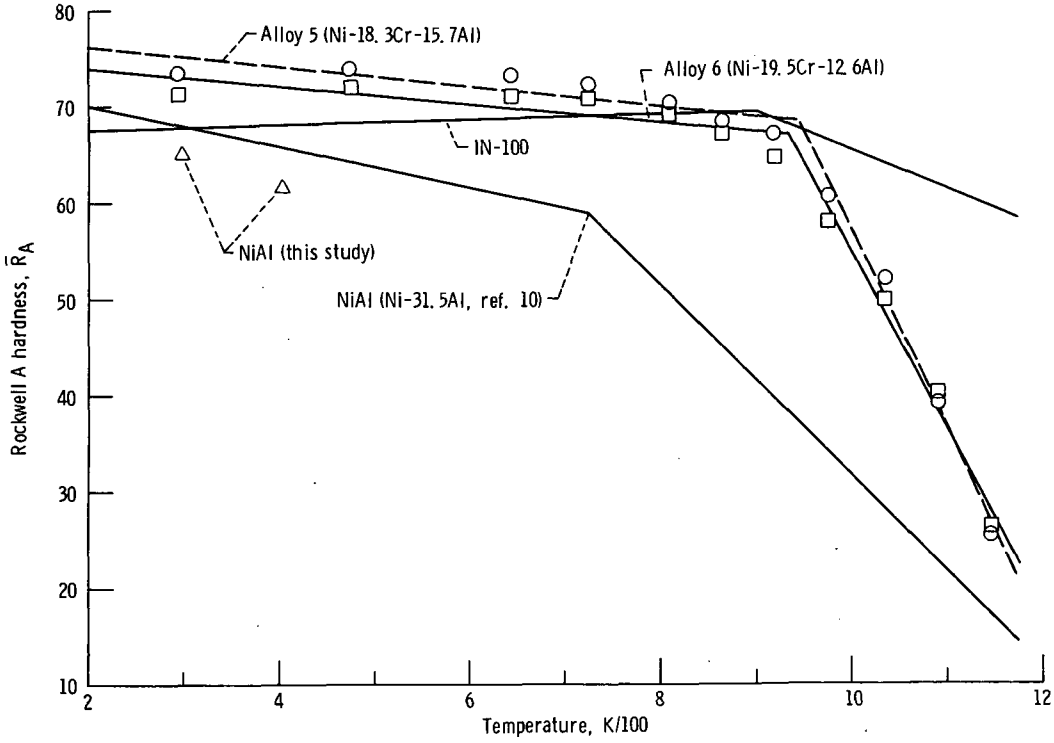

(d) β-rich β + γ NiCrAl alloys and NiAl compared to IN-100.

Figure 3. - Concluded.

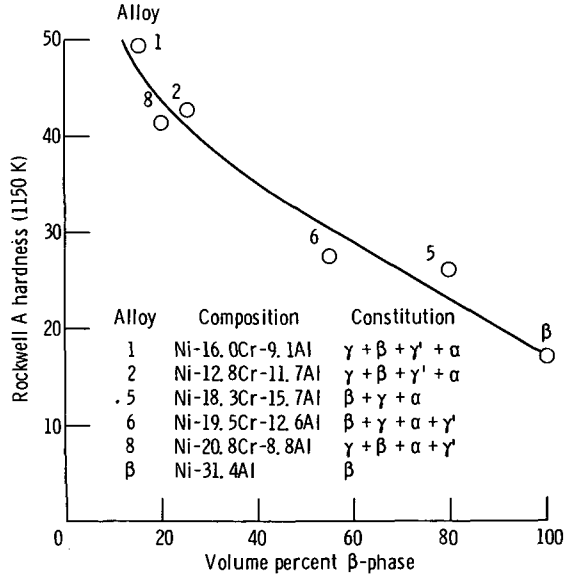

Alloy	Composition	Constitution
1	Ni-16. 0Cr-9. 1Al	γ + β + γ' + α
2	Ni-12. 8Cr-11. 7Al	γ + β + γ' + α
5	Ni-18. 3Cr-15. 7Al	β + γ + α
6	Ni-19. 5Cr-12. 6Al	β + γ + α + γ'
8	Ni-20. 8Cr-8. 8Al	γ + β + α + γ'
β	Ni-31. 4Al	β

Figure 4. - Effect of alloy constitution on 1150 K Rockwell A hardness for β containing alloys.

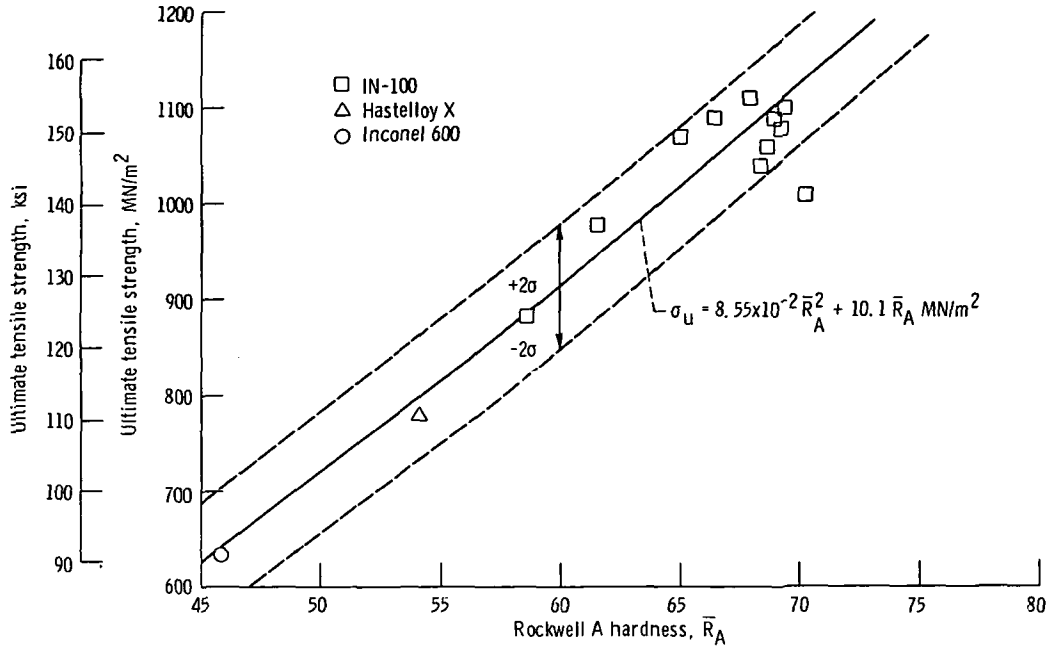

Figure 5. - Ultimate tensile strength as function of Rockwell A hardness for heat resistant nickel alloys.

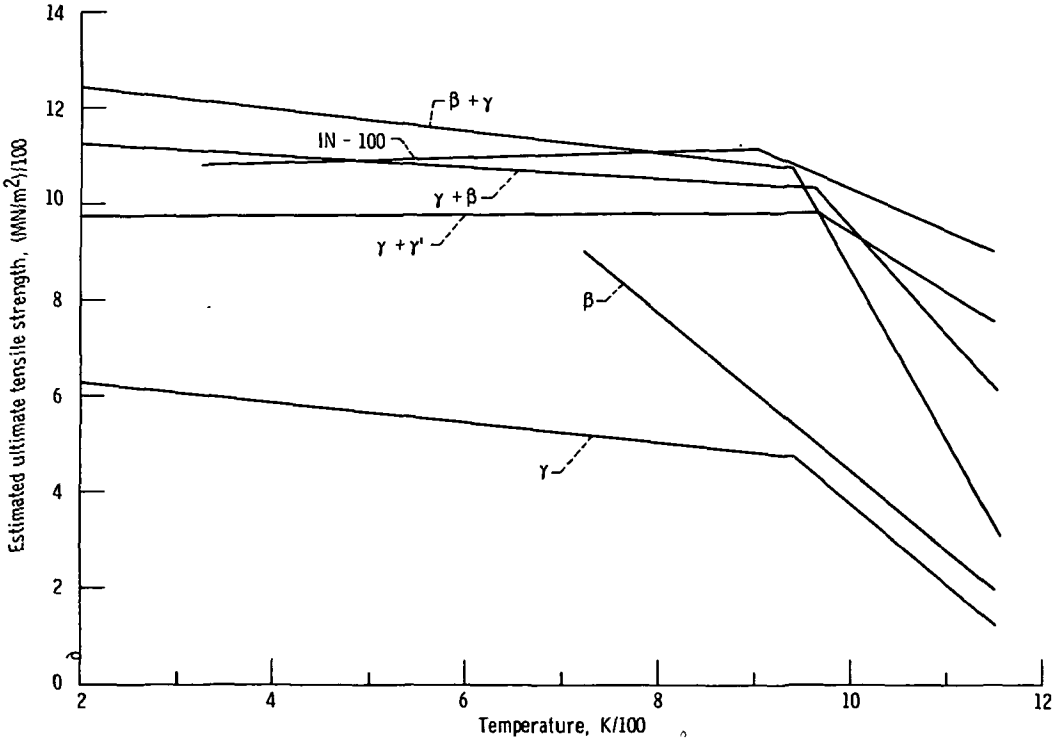

Figure 6. - Average estimated ultimate tensile strength behavior of NiCrAl alloys from hot hardness data.

NATIONAL AERONAUTICS AND SPACE ADMINISTRATION
WASHINGTON, D.C. 20546

OFFICIAL BUSINESS
PENALTY FOR PRIVATE USE $300

SPECIAL FOURTH-CLASS RATE
BOOK

POSTAGE AND FEES PAID
NATIONAL AERONAUTICS AND
SPACE ADMINISTRATION
451

U.S.MAIL

POSTMASTER: If Undeliverable (Section 158 Postal Manual) Do Not Return

"The aeronautical and space activities of the United States shall be conducted so as to contribute . . . to the expansion of human knowledge of phenomena in the atmosphere and space. The Administration shall provide for the widest practicable and appropriate dissemination of information concerning its activities and the results thereof."

—NATIONAL AERONAUTICS AND SPACE ACT OF 1958

NASA SCIENTIFIC AND TECHNICAL PUBLICATIONS

TECHNICAL REPORTS: Scientific and technical information considered important, complete, and a lasting contribution to existing knowledge.

TECHNICAL NOTES: Information less broad in scope but nevertheless of importance as a contribution to existing knowledge.

TECHNICAL MEMORANDUMS: Information receiving limited distribution because of preliminary data, security classification, or other reasons. Also includes conference proceedings with either limited or unlimited distribution.

CONTRACTOR REPORTS: Scientific and technical information generated under a NASA contract or grant and considered an important contribution to existing knowledge.

TECHNICAL TRANSLATIONS: Information published in a foreign language considered to merit NASA distribution in English.

SPECIAL PUBLICATIONS: Information derived from or of value to NASA activities. Publications include final reports of major projects, monographs, data compilations, handbooks, sourcebooks, and special bibliographies.

TECHNOLOGY UTILIZATION PUBLICATIONS: Information on technology used by NASA that may be of particular interest in commercial and other non-aerospace applications. Publications include Tech Briefs, Technology Utilization Reports and Technology Surveys.

Details on the availability of these publications may be obtained from:

SCIENTIFIC AND TECHNICAL INFORMATION OFFICE

NATIONAL AERONAUTICS AND SPACE ADMINISTRATION

Washington, D.C. 20546